The evolution of cylindrical geostrophic vortices

Fernando Viera
School of Mathematics and Statistics
University of Sydney

9 July 1993, revised October 1993

Abstract

The evolution of continuously stratified geostrophic vortices is investigated using a recently developed algorithm. Assuming a three-dimensional vortex region of potential vorticity of arbitrary vertical structure but piecewise-constant distribution in the horizontal direction, the problem is reduced to the Lagrangian evolution of the two-dimensional boundary surface enclosing the vortex region. Simulations of the evolution of elliptical cylinder vortices in a spatially unbounded fluid of uniform stratification are presented. Preliminary findings indicate that for scales large compared to the internal radius of deformation the process of axisymmetrization of the elliptical structure is greately enhanced with no evidence of filamentation.

1. Introduction

In the last decade it has become clear that coherent structures play an important role in the evolution of high Reynolds number turbulent-like flows. The studies of [1, 3] (and references therein) show that coherent structures develop through the process of axisymmetrization of a vorticity patch and then dominate the dynamics of the flow. Relaxation towards axisymmetrization has been studied in detail by Melander *et al.* [4] who showed that in Eulerian and barotropic geostrophic flows, a near elliptical vortex relaxes to axisymmetry as a result of an inviscid mechanism involving filamentation. The merger of two vortices, a phenomenon of fundamental importance in the study of two-dimensional turbulent flows, is also the result of an inviscid process involving relaxation towards axisymmetrization (Melander *et al.* [5]). On the other hand, high resolution simulations of three-dimensional geostrophic turbulence in a continuously stratified fluid by McWilliams [2] have also shown that coherent structures are formed consisting mainly of horizontally axisymmetric vortices.

Motivated by the results of the aformentioned studies, in this article we present preliminary investigations of the evolution of continuously stratified geostrophic vortices of finite height and elliptical cylinder shape immersed in a spatially unbounded fluid. We use the method of boundary surface dynamics, a recently developed algorithm (Viera, [7]) that reduces the dimensionality of the three-dimensional problem by one and hence allows the use of high vertical resolution with reduced computational effort. Here however, we have introduced a node insertion/deletion scheme to extend the integrations further in time and improve computational efficiency. Our principal aim is to identify the conditions which may enhance or inhibit axisymmetrization and the filamentation process.

2. Basic equations

The potential vorticity in large scale fluid motions in the ocean and atmosphere, given by

$$Q(x,y,z) = \psi_{xx} + \psi_{yy} + \gamma^{-2}\psi_{zz}, \tag{2.1}$$

satisfies the conservation law

$$Q_t + uQ_x + vQ_y = 0, \tag{2.2}$$

where $\psi(x,y,z,t)$ is the stream function of the horizontal velocity field such that

$$(u,v) = (-\psi_y, \psi_x),$$

and

$$\gamma = L_D/L, \qquad L_D = \mathcal{N}D/f, \qquad \mathcal{N}^2 = (-g/\rho)\rho_z. \tag{2.3}$$

Here, L_D is the internal radius of deformation, $\mathcal{N}$ is the constant Brunt-Väisälä frequency, f is the Coriolis parameter, $\rho(z)$ the density and L, D are characteristic horizontal and vertical length scales respectively.

We now assume that the potential vorticity field consists of a finite volume V in a spatially unbounded fluid such that

$$Q(x,y,z) = \begin{cases} Q_I(z), & \text{inside } V \\ Q_O(z), & \text{outside } V, \end{cases}$$

where Q_I and Q_O are functions of z only. Then it can be shown ([7]) that the velocity field can be expressed in the form

$$(u,v) = -\frac{1}{4\pi}\iint_S \Delta Q(z')G(\mathbf{r},\mathbf{r}')(dx',dy')dz', \tag{2.4}$$

where S is the closed surface enclosing the volume V,

$$\Delta Q(z') = Q_O(z') - Q_I(z'),$$

and

$$G(\mathbf{r},\mathbf{r}') = [(x-x')^2 + (y-y')^2 + \gamma^2(z-z')^2]^{-\frac{1}{2}},$$

is the Green's function of Laplace's operator on the right hand side of (2.1). The conservation equation (2.2) ensures that the problem is now completely determined by following the evolution of the boundary surface S using the Lagrangian equations

$$\frac{dx}{dt} = u(x,y,z,t), \qquad \frac{dy}{dt} = v(x,y,z,t), \tag{2.5}$$

where the velocity field is evaluated at the surface S. The three-dimensional problem has been reduced to the evolution of the two-dimensional boundary surface of the vortex region V.

3. The numerical algorithm

We write (2.4) in the form

$$(u,v) = -\frac{1}{4\pi}\int_{z_B}^{z_T} \Delta Q(z') M^{(u,v)}(z')dz', \tag{3.1}$$

where

$$M^{(u,v)}(z') = \oint_{\mathcal{C}} G(\mathbf{r},\mathbf{r}')(dx',dy'),$$

and $\mathcal{C}$ is a closed curve obtained by the intersection of S with a horizontal plane $z = z_k, (z_B \le z_k \le z_T)$. The superscripts (u,v) refer to the (x',y')-integrals of the (u,v)-components of the velocity field respectively. The surface S is discretized by a set of points (x_{ik}, y_{ik}, z_k) such that $0 \le i \le N+1$ and $1 \le k \le N_z$, where N_z is the number of z-levels, $N+2$ the number of points on each level and $z_B = z_1$ and $z_T = z_{N_z}$. Using a Gaussian quadrature in the z-direction, the velocity field becomes

$$(u_{ik}, v_{ik}) = -\frac{1}{4\pi}\left\{\frac{1}{2}(z_{N_z} - z_1)\sum_{l=1}^{N_z} W_l \Delta Q(z_l) M^{(u,v)}(z_l) + I_{ik}^{(u,v)}\right\}, \tag{3.2}$$

where W_l are the weights and $M^{(u,v)}(z_l)$ are computed using a trapezoidal rule. The expressions $I_{ik}^{(u,v)}$ are singular integrals over a small surface patch containing the singular point (x_{ik}, y_{ik}, z_k) (see [7] for details of the computations of the singular integrals). The time stepping is performed using a standard fourth-order Runge-Kutta method.

Here, we have improved the algorithm by including a node insertion/deletion scheme on each level to maintain adequate resolution for longer integration times and increase computational efficiency. The scheme is based on that described in [6]. Basically a node is inserted between two consecutive points if their distance $d_i > \epsilon$ where

$$\epsilon = \max[\min(0.1\kappa^{-1}, S_{max}), 0.021], \qquad S_{max} = \min[0.03P, 0.15], \tag{3.3}$$

κ is the local contour curvature, and P the perimeter of the contour. A node is deleted if $d_i < \max[0.02, 0.1\epsilon]$. These parameters were obtained by numerical experimentation and found suitable for the present application.

4. Numerical results

We now consider as initial condition a cylindrical vortex of elliptical cross section $(a\cos\theta, b\sin\theta)$ and unit height with $z_B = -1$ and $z_T = 0$. In all simulations reported here we use $\Delta t = 0.4$ and $N_z = 24$ (except in Figure 5 where $N_z = 32$). The relative change in volume of the final structure remained less than 4%. Initially we take $a = 2$, $b = \frac{1}{2}$ and $\Delta Q = -1$. Whenever ΔQ is independent of z, the evolution is symmetric about the middle plane of the vortex and hence only the lower half (levels 1 to 12) are shown in the figures.

Figures 1, 2 and 3 show the evolution for $\gamma = 1, 0.3, 4$ respectively, at levels $(z_1, z_4, z_7, z_{12}) \approx (-1, -0.9, -0.8, -0.53)$. There is a clear tendency of evolution towards axisymmetrization for $\gamma = 1$, in particular in the inner levels ($k = 7, ..., 11$) where the aspect ratio has decreased from $\lambda = 4$ to $\lambda \approx 2.2$. The bottom level $k = 1$

(and $k = 2,3$ not shown) also show a tendency to axisymmetrize but they eject filamentary arms in the process. For $\gamma = 0.3$ there is a strong tendency towards axisymmetrization with no filamentation present on any level. The aspect ratio at $t = 40$ is now $\lambda \approx 1.5$ which is a reduction of about 63% of the initial value. We recall from (2.3) that small γ implies that the horizontal scale of the motion L is larger than the internal radius of deformation L_D. For $\gamma = 4$ axisymmetrization has been inhibited. There is now greater vertical distortion of the vortex as seen by comparing the four levels at $t = 40$. In Figure 4 we return to $\gamma = 1$ but let $b = \frac{1}{4}$. Reducing the aspect ratio of the initial elliptical cross-section leads to fragmentation of the outer levels of the vortex.

Figure 5 shows the evolution of a cylinder of height 2 with all other parameters as in Figure 1. At $t = 40$, $\lambda \approx 1.3$ in the middle level $k = 16$ with no evidence of filamentation. The outer levels ($k = 1, ..., 5$) also axisymmetrize at $t = 40$ but with long filamentary arms forming after going through an "S" shape stage at $t = 26.7$. Figure 6 shows the evolution of a shorter vortex of height 0.5. Reducing the height has the effect of inhibiting both axisymmetrization and filamentation, giving a "peanut" shaped horizontal cross-section. There is very little distortion in the vertical direction.

The above simulations have assumed a constant value of ΔQ. In the real ocean or atmosphere the potential vorticity is not constant in the vertical direction, but usually varies as a function of z. Hence we now consider the effects of variable Q_I in the vertical with $Q_O = 0$. In Figure 7 we choose the simple linear distribution $Q_I(z) = 1 - z$ and therefore $Q_I(-1) = 2$ and $Q_I(0) = 1$. The larger value of Q_I in the lower levels effectively enhances axisymmetrization and filamentation of the upper parts of the vortex. We point out that the purpose of this idealized distribution is to give some insight into the effects of variable ΔQ. More realistic variations would be required to simulate actual geophysical flows.

5. Summary

Preliminary investigations using the method of boundary surface dynamics indicate that for scales large compared to the internal radius of deformation, the effects of continuous stratification and high vertical resolution enhance the process of evolution towards axisymmetrization with very little filamentation of the vortex structure. Increasing the height of the vortex also increases axisymmetrization, all other parameters being equal. However, decreasing the eccentricity of the elliptical cross section produces an instability leading to horizontal fragmentation of the outer levels of the vortex. Finally, we would like to point out that more numerical experiments are required in order to quantify the nature of the processes involved in these simulations.

References

1. J.C. McWilliams. The emergence of isolated coherent vortices in turbulent flow. *J. Fluid Mech.*, 146:21–43, 1984.
2. J.C. McWilliams. Statistical properties of decaying geostrophic turbulence. *J. Fluid Mech.*, 198:199–230, 1989.
3. J.C. McWilliams. The vortices of two-dimensional turbulence. *J. Fluid Mech.*, 219:361–385, 1990.
4. M.V. Melander, J.C. McWilliams, and N.J. Zabusky. Axisymmetrization and vorticity-gradient intensification of an isolated two-dimensional vortex through filamentation. *J. Fluid Mech.*, 178:137–159, 1987.
5. M.V. Melander, N.J. Zabusky, and J.C. McWilliams. Symmetric vortex merger in two dimensions: causes and conditions. *J. Fluid Mech.*, 195:303–340, 1988.
6. D.I. Pullin and P.A. Jacobs. Inviscid evolution of stretched vortex arrays. *J. Fluid Mech.*, 171:377–406, 1986.
7. F. Viera. Boundary Surface Dynamics: An algorithm for stratified geostrophic flows. *J. Comput. Phys.* , (To appear), 1993.

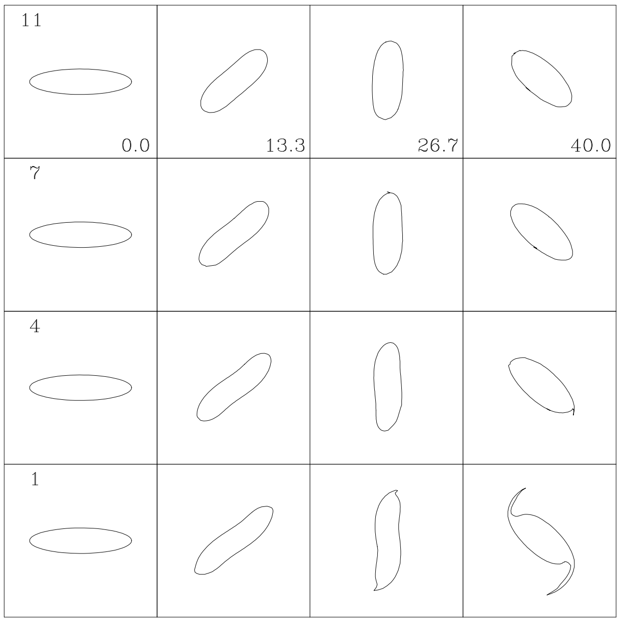

FIGURE 1. The evolution for $\gamma = 1$ at levels $(z_1, z_4, z_7, z_{11}) \approx (-1, -0.9, -0.8, -0.5)$ for $\Delta Q = -1$, $a = 2$ and $b = \frac{1}{2}$. These parameter values apply to all subsequent figures unless otherwise stated.

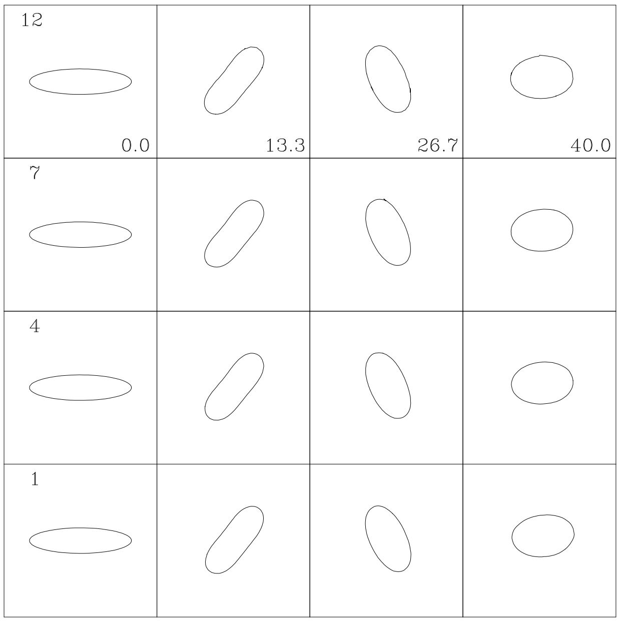

FIGURE 2. The evolution for $\gamma = 0.3$.

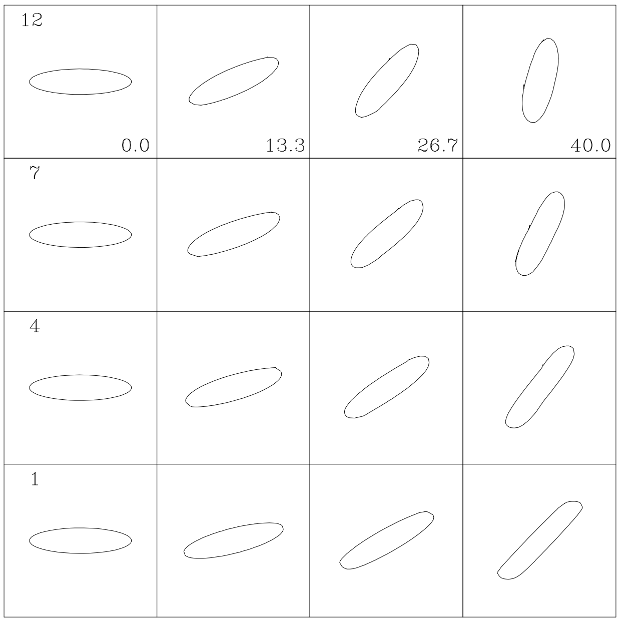

FIGURE 3. The evolution for $\gamma = 4$.

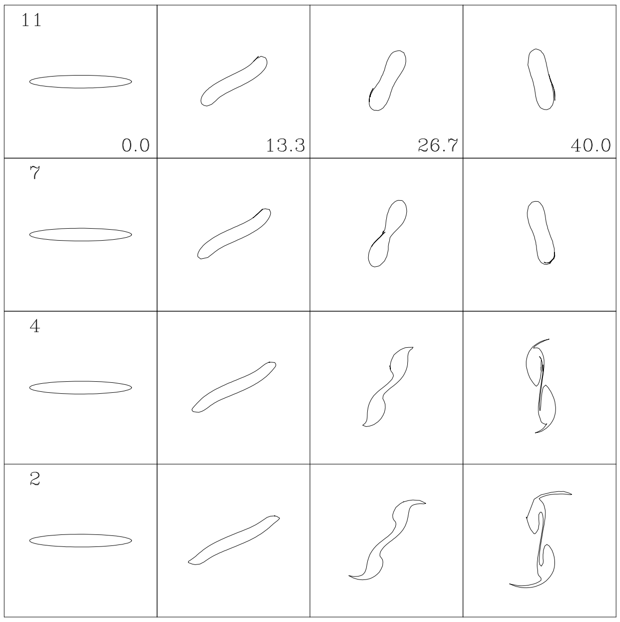

FIGURE 4. The evolution for $\gamma = 1$, $a = 2$ and $b = 0.25$.

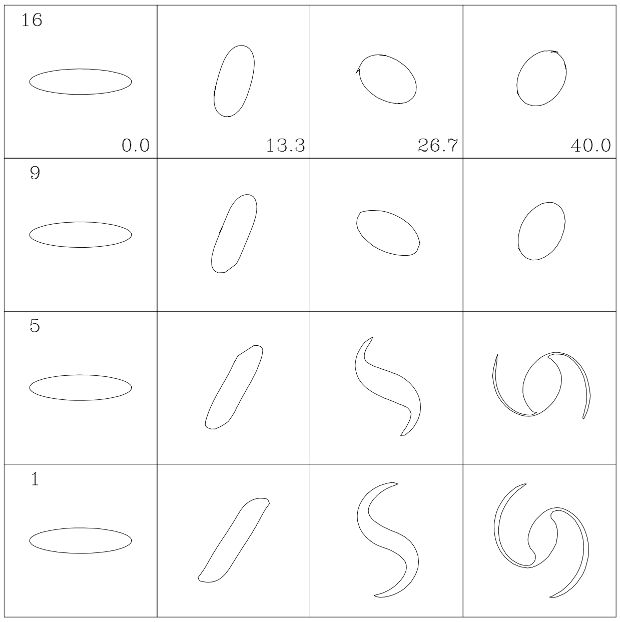

FIGURE 5. The evolution for $\gamma = 1$ and $z_B = -2$.

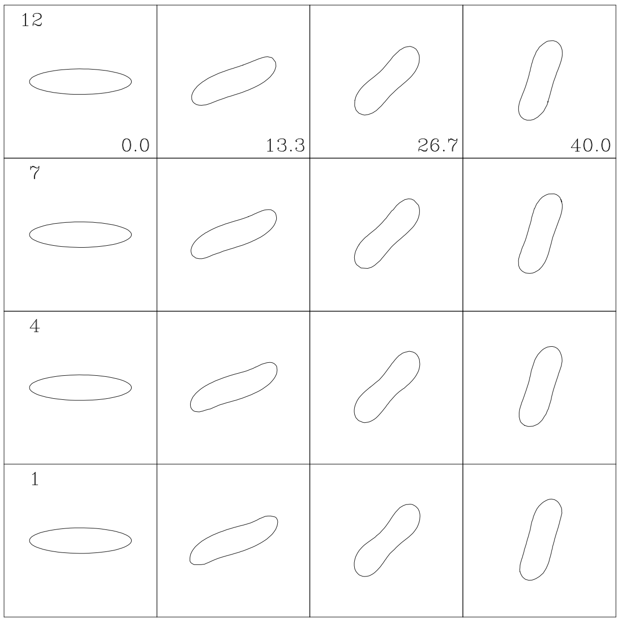

FIGURE 6. The evolution for $\gamma = 1$ and $z_B = -0.5$.

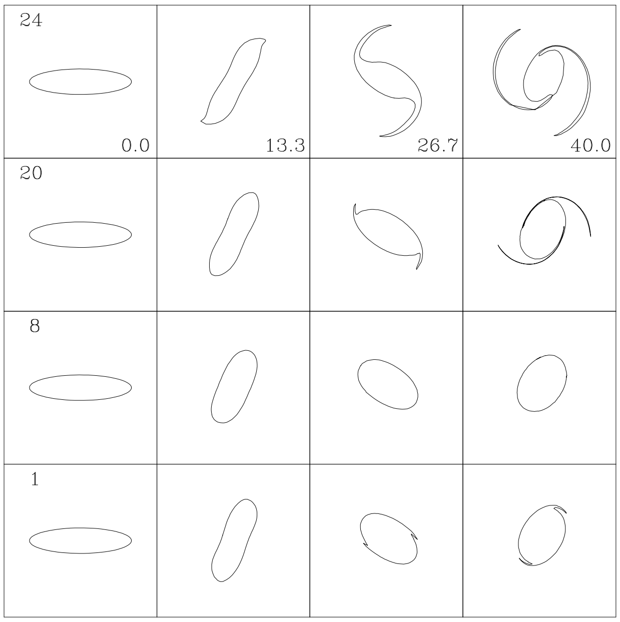

FIGURE 7. The evolution for $\gamma = 1$ and $Q_I = 1 - z$.